NASA TECHNICAL NOTE

NASA TN D-5068

C. 1

NASA TN D-5068

A TECHNIQUE TO INFER ATMOSPHERIC TEMPERATURE FROM HORIZON RADIANCE PROFILES

by Thomas B. McKee, Ruth I. Whitman, and Jules J. Lambiotte, Jr.

Langley Research Center
Langley Station, Hampton, Va.

NATIONAL AERONAUTICS AND SPACE ADMINISTRATION • WASHINGTON, D. C. • FEBRUARY 1969

NASA TN D-5068

A TECHNIQUE TO INFER ATMOSPHERIC TEMPERATURE FROM HORIZON RADIANCE PROFILES

By Thomas B. McKee, Ruth I. Whitman,
and Jules J. Lambiotte, Jr.

Langley Research Center
Langley Station, Hampton, Va.

NATIONAL AERONAUTICS AND SPACE ADMINISTRATION

For sale by the Clearinghouse for Federal Scientific and Technical Information
Springfield, Virginia 22151 – CFSTI price $3.00

A TECHNIQUE TO INFER ATMOSPHERIC TEMPERATURE FROM HORIZON RADIANCE PROFILES

By Thomas B. McKee, Ruth I. Whitman,
and Jules J. Lambiotte, Jr.
Langley Research Center

SUMMARY

A technique is presented to infer atmospheric temperature structure from horizon radiance profiles. The technique was implemented for a spectral region of absorption due to the CO_2 molecule $(615\ cm^{-1}$ to $715\ cm^{-1})$. Inferred temperature accuracy is shown when input data are errorless and when input data have been perturbed with errors for the altitude range from 20.5 km to 55.5 km. Atmospheric temperatures were inferred from measured horizon radiance profiles and compared with estimated temperature structure as an example of the application of the technique to real data.

INTRODUCTION

The objective of the NASA Project Scanner was to measure horizon radiance profiles of the earth which would provide a better understanding of the primary input to horizon sensing devices. Horizon radiance profiles were measured in two spectral bands of the strongly absorbing atmospheric constituents: CO_2 $(615\ cm^{-1}$ to $715\ cm^{-1})$ and H_2O $(315\ cm^{-1}$ to $475\ cm^{-1})$. By using independently determined temperature and pressure conditions of the atmosphere for the same geographical regions these measurements showed excellent agreement with calculated radiance profiles in the CO_2 band when horizontal temperature gradients were low. A description of the project and the measurements for summer conditions are given in reference 1. Measurements for winter conditions are presented in reference 2.

A natural outgrowth of the measurement and the analytic programs to obtain radiance profiles was to reverse the problem and use measured horizon radiance profiles to infer atmospheric characteristics. The CO_2 spectral band is particularly well adapted to temperature inference since the mixing ratio of CO_2 is constant with altitude and is known. This technique therefore is a part of the broad, general topical area of remotely probing

the atmosphere. The favorable geometry which characterizes tangential viewing and leads to its usefulness in atmospheric probing is the same geometry which allows successful atmospheric density determinations from occultation measurements. Considerable effort has been made in remotely probing the atmosphere by viewing in the nadir and measuring radiance as a function of wavelength or frequency. Descriptions illustrative of the nadir viewing problem are given in references 3 to 5.

This paper describes a technique which allows the inference of vertical temperature structure from a measured horizon radiance profile. The derivation and application of the technique are presented for the 615 cm^{-1} to 715 cm^{-1} spectral interval but are not limited to that interval. Sensitivity of the method to various errors is examined for this spectral interval. An example of the application of the method to Project Scanner measured data for the summer conditions is given and compared with the independently estimated temperature structure at that time.

SYMBOLS

C_1	constant, 1.1909×10^{-5} erg-centimeter^2/second-steradian
C_2	constant, 1.4389 centimeters-degrees Kelvin
G	integral ratio
GMT	Greenwich mean time
h	altitude, kilometers
H	tangent height, kilometers
J_ν	source function, watts/meter^2-steradian-centimeter^{-1}
N	radiance, watts/meter^2-steradian
N_c	calculated radiance, watts/meter^2-steradian

N_m	measured radiance, watts/meter^2-steradian
N_ν	spectral radiance, watts/meter^2-steradian-centimeter^{-1}
N_{ν_a}	average spectral radiance, watts/meter^2-steradian-centimeter^{-1}
s	distance along line of sight, kilometers
T	temperature, degrees Kelvin
Γ	lapse rate, -dT/dh, degrees Kelvin/kilometer
ν	wave number, centimeter^{-1}
ν_1	lower limit of integration, centimeter^{-1}
ν_2	upper limit of integration, centimeter^{-1}
ν_a	average wave number, centimeter^{-1}
τ	transmittance

Subscripts:

i	integer
o	values at highest altitude of inferred temperature
1,2,3,4	points along line of sight

DERIVATION

The technique employed to infer atmospheric temperature structure is an iterative process applied to the equation of radiative transfer used to calculate horizon radiance profiles. A discussion of the calculation of radiance profiles and the derivation of the technique for the inference of temperature are presented.

Radiance Profile Calculation

An horizon radiance profile is observed as an instrument outside the atmosphere with a very small optical field of view scans across the horizon (limb). One line of sight through the atmosphere is shown in figure 1. The line of sight is positioned in relation to the earth by its tangent height which is the distance along a radius vector from the surface of the earth to the point where the radius vector is normal to the line of sight. A radiance profile is then radiance as a function of tangent height.

The radiance exiting the atmosphere along a line of sight is given by the equation of radiative transfer (see ref. 6) as

$$N(H) = -\int_{\nu}\int_{s} J_{\nu} \frac{\partial \tau}{\partial s}\, ds\, d\nu + \int_{\nu} J_{\nu}\tau_1\, d\nu \tag{1}$$

Any calculation of a radiance profile must evaluate equation (1) at different tangent heights. The second integral in equation (1) represents a boundary, that is clouds or the surface of the earth, and if the line of sight does not encounter a boundary, the term is not required. In figure 1 the transmittance τ_1 is either to the boundary or to the edge of the atmosphere. For the present problem let the source function be restricted to thermal radiation from gases in the atmosphere; then the source function can be expressed as the ideal Planck radiator where

$$J_{\nu} = N_{\nu} = \frac{C_1 \nu^3}{\exp\left(\frac{C_2 \nu}{T}\right) - 1} \tag{2}$$

With these restrictions equation (1) becomes

$$N(H) = -\int_{\nu}\int_{s} N_{\nu} \frac{\partial \tau}{\partial s}\, ds\, d\nu \tag{3}$$

Usually equation (3) is transformed into an integration over transmittance and wave number and is evaluated from

$$N(H) = -\int_{\nu}\int_{\tau} N_{\nu}\, d\tau\, d\nu \tag{4}$$

Since the Project Scanner measured data are for the 615 cm^{-1} to 715 cm^{-1} region of an absorption band of the CO_2 molecule, the data for this paper are in terms of the 615 cm^{-1} to 715 cm^{-1} spectral region. The technique however is applicable to other spectral regions and other atmospheric components. For the present work the evaluation of equation (1) is described in detail in reference 7. Transmittance data from reference 8 was used, and the mixing ratio of CO_2 was taken to be 314 parts per million at all altitudes. In order to calculate a radiance profile from equation (4) for a given spectral interval, certain atmosphere parameters are needed. The source function N_ν is dependent only on temperature. Transmittance is dependent on geometry, temperature, pressure, and the mixing ratio of CO_2.

The radiance profile for 615 cm^{-1} to 715 cm^{-1} computed from equation (4) by using the 1962 U.S. Standard Atmosphere (ref. 9) is shown in figure 2. The mixing ratio of CO_2 is assumed to be constant throughout the atmosphere; thus the low pressure (and therefore low densities) that exists at high tangent heights results in low radiances. The region of greatest radiance change (between approximately 55 km and 20 km) is due primarily to the increase in pressure (and therefore, the increase in the number of absorbing molecules) along the line of sight as tangent height decreases. Below $H = 20$ km, the profile exhibits small changes in radiance which are a result of the atmosphere becoming opaque.

In order to examine more closely the characteristics of equation (4), which indicate that an iterative technique to obtain temperature from radiance is attractive, the integration is separated into the sum of three integrals along the line of sight so that

$$N(H) = -\int_{\nu_1}^{\nu_2}\int_{1}^{\tau_3} N_\nu \, d\tau \, d\nu - \int_{\nu_1}^{\nu_2}\int_{\tau_3}^{\tau_2} N_\nu \, d\tau \, d\nu - \int_{\nu_1}^{\nu_2}\int_{\tau_2}^{\tau_1} N_\nu \, d\tau \, d\nu \tag{5}$$

When the atmosphere is spherically stratified (as shown in fig. 1), the geometric length along the line of sight is much greater for the first layer τ_3 to τ_2 above the tangent point than for any other layer. In addition to the geometrical factor, the density decreasing exponentially with altitude further emphasizes that most of the atmospheric mass along the line of sight is near the tangent point.

The fractional contribution to equation (5) from the region τ_3 to τ_2 is given by

$$G(H) = \frac{-\int_{\nu}\int_{\tau_3}^{\tau_2} N_\nu \, d\tau \, d\nu}{N(H)} \tag{6}$$

Figure 3 shows $G(H)$ for a 1-km-thick layer as a function of H for the spectral interval 615 cm^{-1} to 715 cm^{-1} and the 1962 U.S. Standard Atmosphere. For tangent

heights above 30 km, the 1-km layer above the tangent point contributes more than 20 percent of the radiance. An iteration technique is attractive when the second integral of equation (5) provides a workable portion of the total radiance $N(H)$ along the line of sight. At $H = 15$ km, the 1-km layer contributes only 3.5 percent of the radiance. At $H = 10$ km, the contribution is less than 0.5 percent, and consequently the technique should be ineffective and highly sensitive to radiance errors at $H = 10$ km for the spectral band considered $\left(615 \text{ cm}^{-1} \text{ to } 715 \text{ cm}^{-1}\right)$.

Temperature Inference

Assumption.- The technique to infer atmospheric temperature structure requires the following three assumptions:

(1) Transmittance model

(2) Knowledge of pressure as a function of altitude

(3) Knowledge of mixing ratio as a function of altitude

The absolute magnitude and accuracy of the deduced temperature is dependent upon the choice of the transmittance model and the accuracy of the pressure and mixing-ratio set. The technique is not dependent on any one transmittance model; therefore the transmittance model used in this study was chosen primarily because of its availability in program form and secondarily because of its general acceptability. The relative merit of any one transmittance model is difficult to determine at the present time and is not the subject of this paper. Pressure as a function of altitude could be chosen, as a first approximation, from model or climatological atmospheric data. The value of 314 parts per million as the mixing ratio for CO_2 is widely accepted and has been used for this study. The technique is not dependent on any given value of mixing ratio but only on the knowledge of the mixing ratio as a function of altitude.

Technique.- The iterative technique to obtain temperature begins at high tangent heights and proceeds downward. The temperature above the highest altitude of an inferred temperature is approximated by a constant lapse rate given by

$$T = \Gamma\left(h - h_0\right) + T_0 \tag{7}$$

The lapse rate is arbitrarily chosen to be representative of a model atmosphere and its effect on the deduced temperatures is soon damped out.

Evaluation of equation (4) with an initially assumed Γ and T_0 will yield the calculated radiance to be

$$N_c(H_o) = -\int_{\nu_1}^{\nu_2}\int_{1}^{\tau_1} N_\nu(T)\,d\tau\,d\nu \tag{8}$$

From the measured radiance profile $N_m(H)$ the radiance error between the calculated and measured values is

$$\Delta N(H_o) = N_m(H_o) - N_c(H_o) \tag{9}$$

At this point it is possible to determine a ΔT and iterate until $\Delta N(H_o)$ is small.

In order to enhance the calculation of a ΔT, equation (8) can be approximated by removing the source function from the integrand and evaluating the source function at an average value of ν, which is $\frac{\nu_1 + \nu_2}{2} = \nu_a$, so that

$$N_c(H_o) = N_{\nu_a}(T_o)\int_{\nu_1}^{\nu_2}\int_{1}^{\tau_1} d\tau\,d\nu \tag{10}$$

Since τ depends only slightly on T, an approximation to the change in radiance with a change in temperature is

$$\frac{\Delta N}{\Delta T} \approx \frac{\partial N_{\nu_a}(T_o)}{\partial T}\int_{\nu_1}^{\nu_2}\int_{1}^{\tau} d\tau\,d\nu \tag{11}$$

A further approximation from equation (2) is useful in equation (11) since

$$\frac{\partial N_\nu}{\partial T} = N_\nu(T)\frac{C_2\nu}{T^2}\left(\frac{\exp\frac{C_2\nu}{T}}{\exp\frac{C_2\nu}{T} - 1}\right) \tag{12}$$

For the present problem $C_2 = 1.4389$ cm-^oK, $\nu_a = 665$ cm^{-1}, and $200^o\ K \leqq T \leqq 300^o\ K$ or $24 \leqq \exp\frac{C_2\nu}{T} \leqq 118$. Since $\exp\frac{C_2\nu}{T} - 1 \approx \exp\frac{C_2\nu}{T}$, the factor $\frac{\exp\frac{C_2\nu}{T}}{\exp\frac{C_2\nu}{T} - 1}$ in equation (12) reduces to unity. This approximation would simplify equation (11) to

$$\frac{\Delta N}{\Delta T} = N_{\nu_a}(T_o)\frac{C_2\nu_a}{T_o^2}\int_{\nu_1}^{\nu_2}\int_1^{\tau_1} d\tau\, d\nu \tag{13}$$

Now the substitution of equation (13) in equation (9) yields

$$\Delta T = \frac{\left[N_m(H_o) - N_c(H_o)\right]T_o^2}{N_{\nu_a}(T_o)C_2\nu_a\int_{\nu_1}^{\nu_2}\int_1^{\tau_1} d\tau\, d\nu} \tag{14}$$

The use of equation (14) in sequence with equation (8) until ΔN is small indicates that the temperatures at $h = h_o$ and above have been determined.

The calculation proceeds to the next lower tangent height at $H = H_i$ and evaluates equation (5) by using T_i for the new layer equal to the temperature in the layer immediately above the ith layer. In equation (5) the first integral is completely determined since the temperatures above the ith layer have been previously determined. The second integral is not known and is strongly dependent on the temperature of the new layer which lies between τ_3 and τ_2 along the line of sight. Changing temperature in the new layer will have a small effect on the third integral in that τ_2 and τ_1 are slightly dependent on the temperature in the ith layer. The temperature of the new ith layer is changed until the difference between calculated and measured radiance at H_i is small. The estimate of the ΔT required is similar to equation (14) except only the limits of τ_3 to τ_2 are needed. The expression is

$$\Delta T_i = \frac{\left[N_m(H_i) - N_c(H_i)\right]T_i^2}{N_{\nu_a}(T_i)C_2\nu_a\int_{\nu_1}^{\nu_2}\int_{\tau_3}^{\tau_2} d\tau\, d\nu} \tag{15}$$

The use of equations (5) and (15) in sequence until $\Delta N(H_i)$ is small indicates that the temperature at h_i has been determined. The calculation then proceeds to the next tangent height and thus works down through the atmosphere layer by layer.

Constants.- For all results presented, $h_o = 60.5$ km and $\Gamma = 3^o$ K/km. In order to restrict the number of iterations, ΔN was considered to be sufficiently small, and thus a solution was considered to have been determined when $\Delta N \leq 0.001$ W/m^2-sr or when $\Delta T \leq 0.5^o$ K. The iterative technique was allowed 5 km to settle out errors from the initial assumptions inherent in equation (7), and therefore the inferred temperatures from 60.5 km to 55.5 km have not been included in the results.

EVALUATION OF TECHNIQUE

The evaluation of the technique to infer temperature proceeds by inferring temperature from perfect (errorless) radiance data calculated from the 1962 U.S. Standard Atmosphere (fig. 2) and then by inferring temperature with data perturbed with errors which are most likely to be encountered in a measurement. Examination of the temperature profiles inferred from the perturbed data reveals the sensitivity of the method to radiance errors, tangent height errors, and errors in assumed pressure structure. Radiance errors are separated into three types normally found in a measurement; they are sensitivity or multiplicative errors (scale), additive errors (bias), and random errors (noise). Errors associated with the transmittance model and the mixing-ratio assumption were not investigated.

Temperatures inferred from errorless radiance data calculated from the 1962 U.S. Standard Atmosphere are given in table I and illustrated in figure 4. The temperatures inferred were very accurate for the altitude range investigated (20.5 km to 55.5 km). The larger errors above $h = 48.5$ km for this perfect case are due to the assumption of a lapse rate of 3° K/km above $h = 60.5$ km. Temperature errors are also presented in table I. The temperature errors are quite small, and the condition used to stop the iteration is usually $\Delta T < 0.5^{\circ}$ K.

The sources and values of the errors applied to the perfect data are given in the following table:

Scale error, percent	Bias error, W/m^2-sr	Noise error, W/m^2-sr	Tangent height error, km	Pressure error, percent
±1	±0.01	0.01	0.5	±10
±2	-----	.02	±1.0	---
±3	±.03	----	±2.0	---
±4	-----	.04	----	---
±5	±.05	----	----	---

Inferred temperature errors caused by these errors are given in tables II to VI, and examples are shown in figure 5. All temperature errors are with respect to the 1962 U.S. Standard Atmosphere. The mean, standard deviation, and root mean square of the errors are given in each table and provide statistical measures of the sensitivity of the technique to error.

The inferred temperature profiles for 5-percent and -5-percent scale errors are compared with the 1962 U.S. Standard Atmosphere in figure 5(a). In the inferred temperature profiles the lapse rate (slope) is very accurately determined and the altitudes at which

the slope changes are correctly identified. The lapse rate from $h = 35$ km to $h = 46$ km for the 1962 U.S. Standard Atmosphere is 2.76° K/km and for the inferred structure is 2.70° K/km for a -5-percent scale error and 2.83° K/km for a 5-percent scale error.

Bias errors (fig. 5(b)) cause temperature errors which increase with increasing altitude. A bias error of 0.05 W/m^2-sr is 10.8 percent of the radiance at 55 km but only 2.1 percent of the radiance at 40 km.

The inferred temperature profile oscillates in response to noise radiance errors. Noise radiance errors are illustrated in figure 5(c). The noise source in the radiance error was assumed to be random with a mean of zero and the standard deviation σ given in table IV. The temperature errors are large at higher altitudes and decrease as the radiance error becomes a smaller fraction of the radiance; however, as the fraction of total radiance in the narrow layer above the tangent point decreases (fig. 3), the temperature errors increase at lower altitudes.

Effects of tangent height errors are shown in figure 5(d). Temperature errors are largest at the higher altitudes. The lapse rates from 20 km to 45 km are incorrectly inferred as the inferred temperature profile crosses the reference temperature profile. Lapse rates for the regions $h = 35$ km to $h = 46$ km are -3.08° K/km for a 1-km tangent height error and -2.46° K/km for a -1-km tangent height error.

Deduced temperature errors caused by pressure errors (table VI) are very similar to the temperature errors caused by tangent height errors — for isothermal atmospheres they would be identical. A 10-percent error in pressure causes a little less error than a 1-km tangent height error.

TEMPERATURE INFERENCE FROM MEASURED HORIZON RADIANCE PROFILES

Horizon radiance profiles have been measured in the 615 cm^{-1} to 715 cm^{-1} spectral region in the NASA Project Scanner. A description of the summer measured radiance data, meteorological conditions at the time of measurement, and the application of the temperature inference technique to the summer data are presented.

Summer Measured Horizon Radiance Profiles

The horizon radiance profiles were measured with instrumentation on a rocket probe launched from the NASA Wallops Station at 0618 GMT on August 16, 1966 (ref. 1). Peak altitude attained in the flight was 620 km. Measured horizon radiance profiles were grouped into seven geographic cells. The location of these cells and the number of profiles are given in the following table:

Cell	Latitude	Longitude	Number of profiles
1	58° N	68° W	5
2	53° N	60° W	5
3	47° N	57° W	3
4	43° N	45° W	8
5	35° N	48° W	10
6	21° N	55° W	16
7	17° N	60° W	3

Radiance profiles for these cells are given in table VII. Experimental accuracy of these data are dependent on radiance magnitude; however, approximate values which place the data with respect to the error sensitivity previously discussed are scale errors of ±4 percent, bias errors of ±0.06 W/m^2-sr, and tangent height errors of ±1.3 km. The noise error is dependent on the number of profiles in a given geographic cell. The standard deviation of the noise error for one radiance profile is 0.06 W/m^2-sr. The standard deviation of the noise for one radiance profile is 0.06 W/m^2-sr but this standard deviation decreases as the square root of the number of profiles in the cell. As an example, cell 6 has 16 profiles and therefore the standard deviation of the noise is 0.015 W/m^2-sr, whereas cell 7 with three profiles has a noise error of 0.035 W/m^2-sr.

Meteorological Data

In Project Scanner an attempt was made to determine independently the significant atmospheric temperatures and pressures at a time near the measurement. Seven model atmospheres, one for each geographic cell, are given in table VIII. A discussion of the data used in developing these model atmospheres is given in appendix B of reference 1. Balloon measurements of temperature and pressure were used from the surface to an altitude of 30 km or as high as data were available. No measurements were made for cell 6 which was assumed to have the same data as those measured from the balloon in cell 7. Above 30 km, temperatures were estimated from the wind and temperature measurements from rocketsondes at Fort Churchill, Canada, Wallops Island, Virginia, Eglin Air Force Base, Florida, and White Sands Missile Range, New Mexico. (Wind data were not obtained at White Sands Missile Range.) If balloon temperature data ceased before h = 30 km, the temperature was linearly interpolated to the estimated temperature at 30 km. Pressures for altitudes above the 30-mb level were calculated by hydrostatic buildup by using the pressure at the 30-mb level as a base since pressures below that altitude were available from the balloon measurements. These temperature profiles, which are compared with the temperature profiles inferred from the radiance measurements, serve as an independent estimate.

Inferred Temperature Profiles

Temperature profiles inferred from the radiance profiles in table VII are compared with temperatures of the model atmospheres of table VIII in figure 6. The pressure distributions assumed are those given in table VIII. Temperatures have been inferred at 1-km spacings from $h = 20.5$ km to $h = 55.5$ km. Above $h = 50$ km the accuracy of temperature values is poor relative to the accuracy at lower altitudes. The lapse rates from $h = 30$ km to $h = 45$ km are in good agreement for all data. The inferred temperatures compare favorably with the temperature structure estimated independently. When the accuracy of inferred temperature due to radiance errors is considered, comparisons of data in the 20-km to 30-km altitude range where balloon data were available agree quite well.

The achievable accuracy of inferred temperatures depends upon the magnitudes of the errors experienced in radiance, tangent height, and pressure errors. Accuracy of measured radiances of 1 percent in scale, 0.01 W/m^2-sr in bias, and 0.01 W/m^2-sr in noise is possible in a precise measurement. Inferred temperature errors caused by errors in tangent height and assumed pressure structure should be considerably larger than those due to radiance errors. Future research to refine the present technique should attempt to reduce the dependence or sensitivity to tangent height and pressure errors. One approach could be to infer temperature directly as a function of pressure and eliminate knowledge of tangent height.

CONCLUDING REMARKS

A technique to infer atmospheric temperature structure from horizon radiance profiles has been presented. The technique was implemented for the 615 cm^{-1} to 715 cm^{-1} spectral band of CO_2. Temperature inference of the 1962 U.S. Standard Atmosphere was very accurate for the range of altitudes investigated (20.5 km to 55.5 km) when the radiance profile and the assumed pressure structure contained no errors. The effects of scale, bias, and noise errors in radiance, tangent height errors, and pressure errors are demonstrated.

Atmospheric temperatures were inferred from measured horizon radiance profiles as an example of the application of the technique to measured data in the altitude range of 20.5 km to 55.5 km. The inferred temperatures compare favorably with temperature structures estimated independently.

Langley Research Center,
National Aeronautics and Space Administration,
Langley Station, Hampton, Va., November 21, 1968,
715-02-00-01-23.

REFERENCES

1. McKee, Thomas B.; Whitman, Ruth I.; and Davis, Richard E.: Infrared Horizon Profiles for Summer Conditions From Project Scanner. NASA TN D-4741, 1968.

2. Whitman, Ruth I.; McKee, Thomas B.; and Davis, Richard E.: Infrared Horizon Profiles for Winter Conditions From Project Scanner. NASA TN D-4905, 1968.

3. Wark, D. Q.; and Fleming, H. E.: Indirect Measurements of Atmospheric Temperature Profiles From Satellites: I. Introduction. Mon. Weather Rev., vol. 94, no. 6, June 1966, pp. 351-362.

4. King, Jean I. F.: Meteorological Inferences From Satellite Radiometry, I. J. Atmos. Sci., vol. 20, no. 4, July 1963, pp. 245-250.

5. Conrath, Barney J.: Inverse Problems in Radiative Transfer: A Review. NASA TM X-55857, 1967.

6. Goody, R. M.: Atmospheric Radiation I.- Theoretical Basis. Clarendon Press (Oxford), 1964.

7. Bates, Jerry C.; Hanson, David S.; House, Fred B.; Carpenter, Robert O'B.; and Gille, John C.: The Synthesis of 15μ Infrared Horizon Radiance Profiles From Meteorological Data Inputs. NASA CR-724, 1967.

8. Stull, V. R.; Wyatt, P. J.; and Plass, G. N.: Infrared Transmission Studies. Final Report, Volume III – The Infrared Absorption of Carbon Dioxide. SSD-TDR-62-127, Vol. III, U.S. Air Force, Jan. 31, 1963.

9. Anon.: U.S. Standard Atmosphere, 1962. NASA, U.S. Air Force, and U.S. Weather Bur., Dec. 1962.

TABLE I.- INFERRED TEMPERATURES AND TEMPERATURE ERRORS FOR PERFECT RADIANCE DATA

[Calculated from 1962 U.S. Standard Atmosphere]

Altitude, km	Inferred temperature, °K	Temperature error, °K
20.5	217.12	-0.01
21.5	218.09	.00
22.5	219.07	.00
23.5	220.09	.03
24.5	221.05	-.01
25.5	222.05	.01
26.5	223.05	.01
27.5	224.03	.00
28.5	225.16	.14
29.5	226.01	.00
30.5	227.02	.01
31.5	227.97	-.03
32.5	229.78	-.02
33.5	232.41	-.02
34.5	235.13	.00
35.5	237.92	.02
36.5	240.70	.03
37.5	243.45	.01
38.5	246.24	.04
39.5	248.97	.00
40.5	251.71	-.02
41.5	254.55	.05
42.5	257.30	.04
43.5	260.08	.06
44.5	262.73	-.05
45.5	265.52	-.03
46.5	267.69	-.17
47.5	269.70	-.01
48.5	270.32	-.33
49.5	270.32	-.33
50.5	270.32	-.33
51.5	270.32	-.33
52.5	269.61	-.27
53.5	267.89	-.44
54.5	266.05	-.53
55.5	263.83	-.78
Mean error		-0.09
Root-mean-square error		.21
Standard deviation		.19

TABLE II.- TEMPERATURE ERRORS FOR SCALE RADIANCE ERRORS

Altitude, km	Temperature error, °K, for scale error of –									
	-5%	-4%	-3%	-2%	-1%	1%	2%	3%	4%	5%
20.5	-2.62	-2.09	-1.57	-1.04	-0.52	0.50	1.02	1.53	2.04	2.54
21.5	-2.57	-2.05	-1.53	-1.02	-.50	.51	1.02	1.52	2.02	2.52
22.5	-2.54	-2.02	-1.51	-1.00	-.50	.50	1.00	1.49	1.99	2.48
23.5	-2.47	-1.97	-1.46	-.96	-.46	.53	1.02	1.51	1.99	2.48
24.5	-2.48	-1.98	-1.48	-.98	-.49	.48	.97	1.46	1.94	2.41
25.5	-2.45	-1.95	-1.46	-.97	-.48	.49	.98	1.46	1.93	2.41
26.5	-2.44	-1.95	-1.45	-.96	-.47	.49	.97	1.45	1.93	2.40
27.5	-2.45	-1.95	-1.46	-.97	-.48	.49	.97	1.45	1.92	2.40
28.5	-2.33	-1.83	-1.33	-.84	-.35	.62	1.11	1.59	2.07	2.55
29.5	-2.49	-1.98	-1.48	-.98	-.49	.49	.98	1.47	1.95	2.43
30.5	-2.50	-1.99	-1.48	-.98	-.48	.51	1.01	1.50	1.99	2.47
31.5	-2.57	-2.05	-1.54	-1.03	-.52	.48	.98	1.48	1.97	2.46
32.5	-2.62	-2.09	-1.57	-1.05	-.53	.49	1.00	1.51	2.01	2.51
33.5	-2.68	-2.14	-1.60	-1.07	-.54	.51	1.04	1.56	2.07	2.59
34.5	-2.73	-2.17	-1.62	-1.07	-.53	.54	1.09	1.62	2.15	2.67
35.5	-2.78	-2.21	-1.64	-1.08	-.52	.58	1.14	1.68	2.23	2.77
36.5	-2.84	-2.26	-1.68	-1.10	-.53	.60	1.17	1.73	2.29	2.84
37.5	-2.93	-2.33	-1.74	-1.15	-.56	.60	1.18	1.76	2.33	2.90
38.5	-2.97	-2.36	-1.75	-1.15	-.55	.63	1.24	1.83	2.41	2.99
39.5	-3.08	-2.46	-1.83	-1.21	-.60	.61	1.23	1.83	2.43	3.02
40.5	-3.17	-2.53	-1.89	-1.26	-.63	.61	1.24	1.86	2.47	3.08
41.5	-3.17	-2.51	-1.86	-1.22	-.57	.69	1.34	1.97	2.60	3.22
42.5	-3.25	-2.58	-1.92	-1.25	-.60	.69	1.36	2.00	2.64	3.28
43.5	-3.32	-2.63	-1.95	-1.27	-.59	.73	1.42	2.08	2.74	3.39
44.5	-3.43	-2.74	-2.05	-1.37	-.70	.62	1.31	1.97	2.63	3.28
45.6	-3.46	-2.76	-2.06	-1.37	-.68	.66	1.36	2.03	2.70	3.36
46.5	-3.63	-2.92	-2.22	-1.52	-.82	.53	1.24	1.91	2.59	3.26
47.5	-3.56	-2.84	-2.13	-1.42	-.71	.69	1.38	2.07	2.76	3.44
48.5	-3.72	-3.01	-2.30	-1.60	-.90	.39	1.16	1.83	2.51	3.17
49.5	-3.72	-3.01	-2.30	-1.60	-.90	.39	1.16	1.83	2.51	3.17
50.5	-3.72	-3.01	-2.30	-1.60	-.90	.39	1.16	1.83	2.51	3.17
51.5	-3.72	-3.01	-2.30	-1.60	-.90	.39	1.16	1.83	2.51	3.17
52.5	-3.62	-2.91	-2.21	-1.51	-.82	.44	1.22	1.89	2.55	3.21
53.5	-3.74	-3.03	-2.32	-1.62	-.93	.29	1.12	1.80	2.47	3.14
54.5	-3.82	-3.09	-2.37	-1.66	-.96	.23	1.10	1.78	2.45	3.11
55.5	-3.93	-3.20	-2.48	-1.77	-1.06	.01	.98	1.66	2.33	2.98
Mean error	-3.04	-2.43	-1.83	-1.23	-0.63	0.51	1.13	1.72	2.30	2.87
Root-mean-square error . .	3.08	2.47	1.86	1.26	.66	.53	1.14	1.73	2.31	2.89
Standard deviation	.51	.42	.34	.26	.18	.14	.13	.20	.28	.35

TABLE III.- TEMPERATURE ERRORS FOR BIAS RADIANCE ERRORS

Altitude, km	Temperature error, °K, for bias error of –					
	-0.05 W/m²-sr	-0.03 W/m²-sr	-0.01 W/m²-sr	0.01 W/m²-sr	0.03 W/m²-sr	0.05 W/m²-sr
20.5	-0.24	-0.14	-0.04	0.03	0.11	0.18
21.5	-.22	-.13	-.03	.04	.11	.19
22.5	-.23	-.13	-.03	.04	.11	.18
23.5	-.20	-.10	.00	.07	.14	.21
24.5	-.24	-.14	-.03	.04	.10	.17
25.5	-.32	-.13	-.02	.04	.11	.17
26.5	-.16	-.15	-.02	.05	.11	.17
27.5	-.16	-.16	-.03	.04	.11	.17
28.5	-.03	-.12	.11	.18	.24	.31
29.5	-.18	-.10	-.03	.04	.11	.17
30.5	-.17	-.09	-.02	.06	.13	.20
31.5	-.22	-.13	-.06	.02	.10	.17
32.5	-.23	-.14	-.06	.03	.10	.18
33.5	-.24	-.14	-.05	.04	.12	.21
34.5	-.24	-.13	-.04	.06	.15	.24
35.5	-.24	-.12	-.02	.09	.18	.28
36.5	-.25	-.13	-.02	.10	.20	.31
37.5	-.30	-.16	-.04	.09	.20	.32
38.5	-.31	-.15	-.02	.12	.25	.38
39.5	-.38	-.21	-.07	.09	.23	.38
40.5	-.45	-.26	-.09	.08	.24	.41
41.5	-.43	-.21	-.03	.16	.33	.53
42.5	-.50	-.26	-.06	.16	.36	.57
43.5	-.55	-.28	-.05	.20	.42	.67
44.5	-.73	-.43	-.18	.10	.34	.63
45.5	-.79	-.46	-.16	.14	.39	.74
46.5	-1.03	-.63	-.53	.02	.31	.71
47.5	-1.06	-.69	-.38	.09	.28	.98
48.5	-1.29	-.46	-.55	.12	.75	.91
49.5	-1.29	-1.24	-.55	.12	.75	.91
50.5	-2.01	-1.24	-.55	.12	.75	.91
51.5	-2.01	-1.24	-.55	.12	.75	.91
52.5	-2.28	-1.36	-.54	.26	.98	1.69
53.5	-2.77	-1.66	-.71	.21	1.08	1.93
54.5	-3.36	-2.12	-.85	.30	1.36	2.38
55.5	-4.94	-2.57	-1.33	.33	1.63	2.90
Mean error	-0.83	-0.49	-0.21	0.11	0.38	0.62
Root-mean-square error . .	1.35	.79	.37	.13	.53	.89
Standard deviation	1.06	.61	.31	.08	.38	.64

Table IV.- TEMPERATURE ERRORS FOR NOISE RADIANCE ERRORS

Altitude, km	Temperature error, °K, for noise error of –		
	$\sigma = 0.01$ W/m^2-sr	$\sigma = 0.02$ W/m^2-sr	$\sigma = 0.04$ W/m^2-sr
20.5	2.30	-1.81	-2.91
21.5	-1.37	2.85	9.35
22.5	-.11	-.66	1.34
23.5	-.52	-.78	-4.06
24.5	1.86	-.21	-1.67
25.5	-1.05	-1.21	2.14
26.5	.58	1.53	-1.25
27.5	-.41	2.95	-4.54
28.5	-.33	-.77	-.35
29.5	.06	-.01	-1.34
30.5	.86	-1.00	2.74
31.5	-.13	-.79	-2.38
32.5	-.36	.17	.90
33.5	-.08	-1.76	1.21
34.5	.57	-.62	-.06
35.5	.56	1.90	-5.06
36.5	-.76	1.64	1.95
37.5	-1.12	-.16	2.96
38.5	.17	.44	1.92
39.5	.60	.25	-2.00
40.5	.65	2.04	-1.10
41.5	.44	-3.01	-1.52
42.5	.64	1.92	.81
43.5	-2.12	1.65	2.98
44.5	1.05	-3.34	-1.73
45.5	-.27	3.23	.22
46.5	1.01	-.49	2.78
47.5	.13	.59	-3.85
48.5	.09	-4.99	1.02
49.5	-1.86	3.43	.23
50.5	.93	-.13	4.12
51.5	-1.68	-7.90	-3.66
52.5	3.57	.21	2.21
53.5	-1.75	1.76	14.49
54.5	1.50	.33	-3.28
55.5	-1.82	12.64	-31.55
Mean error	0.05	0.27	-0.53
Root-mean-square error . . .	1.21	3.08	6.45
Standard deviation	1.21	3.07	6.43

TABLE V.- TEMPERATURE ERRORS FOR TANGENT HEIGHT ERRORS

Altitude, km	Temperature error, °K, for tangent height error of –				
	-2 km	-1 km	0.5 km	1 km	2 km
20.5	5.28	2.56			
21.5	4.32	2.74	-1.35	-2.74	
22.5	4.30	1.77	-1.13	-2.28	-4.85
23.5	3.31	2.17	-1.00	-2.05	-4.20
24.5	3.28	1.18	-.82	-1.65	-3.63
25.5	2.29	1.64	-.75	-1.53	-3.11
26.5	1.84	.65	-.58	-1.17	-2.65
27.5	.34	.77	-.48	-.93	-2.08
28.5	-.66	-.22	-.14	-.43	-1.34
29.5	-1.65	-.09	.05	.10	-.45
30.5	-1.96	-1.08	.32	.62	.72
31.5	-1.39	-.91	.54	1.10	1.72
32.5	-1.47	-.51	.44	.90	2.04
33.5	-2.19	-1.00	.26	.52	1.46
34.5	-2.90	-1.22	.53	1.04	1.59
35.5	-3.63	-1.71	.68	1.32	2.39
36.5	-4.27	-1.96	.95	1.86	3.19
37.5	-4.92	-2.38	1.07	2.11	4.00
38.5	-5.51	-2.60	1.31	2.56	4.74
39.5	-6.02	-3.03	1.31	2.78	5.41
40.5	-6.61	-3.13	1.60	3.19	6.09
41.5	-7.35	-3.57	1.71	3.34	6.68
42.5	-7.98	-3.90	1.98	3.88	7.31
43.5	-8.10	-4.24	2.19	4.27	8.33
44.5	-8.52	-3.98	2.22	4.43	8.74
45.5	-9.64	-4.81	2.06	4.10	8.77
46.5	-10.97	-5.16	2.37	4.88	9.15
47.5	-13.39	-6.31	2.51	4.93	10.31
48.5	-14.32	-7.24	3.11	6.96	11.73
49.5	-14.32	-7.24	3.80	6.96	13.85
50.5	-14.97	-7.24	3.80	6.96	14.87
51.5	-16.30	-8.02	3.10	6.96	14.87
52.5	-17.59	-8.55	3.88	7.73	15.03
53.5	-18.59	-9.69	4.17	8.42	16.57
54.5	-19.11	-10.18	4.67	9.39	18.33
55.5	-19.02	-10.33	4.70	9.54	19.76
Mean error	-6.07	-2.97	1.40	2.80	5.75
Root-mean-square error . .	9.45	4.77	2.22	4.45	8.94
Standard deviation	7.25	3.74	1.72	3.46	6.85

Table VI.- TEMPERATURE ERROR FOR 10-PERCENT PRESSURE ERROR

Altitude, km	Temperature error, ^{o}K
20.5	1.52
21.5	1.25
22.5	.99
23.5	.82
24.5	.60
25.5	.45
26.5	.28
27.5	.05
28.5	-.08
29.5	-.54
30.5	-.87
31.5	-1.27
32.5	-1.63
33.5	-1.98
34.5	-2.29
35.5	-2.59
36.5	-2.87
37.5	-3.17
38,5	-3.41
39.5	-3.71
40.5	-3.99
41.5	-4.18
42.5	-4.48
43.5	-4.92
44.5	-5.05
45.5	-5.09
46.5	-5.38
47.5	-5.38
48.5	-5.79
49.5	-5.79
50.5	-5.79
51.5	-5.79
52.5	-5.68
53.5	-5.59
54.5	-6.32
55.5	-6.59
Mean error	-2.90
Root-mean-square error . .	3.87
Standard deviation	2.57

TABLE VII.- SUMMER MEASURED RADIANCE PROFILES

FROM PROJECT SCANNER

[From ref. 1]

Tangent height, km	Radiance, W/m^2-sr, for cell –						
	1	2	3	4	5	6	7
10	5.91	5.90	5.85	5.73	5.49	5.45	5.23
11	5.93	5.92	5.85	5.75	5.52	5.46	5.24
12	5.95	5.94	5.85	5.77	5.54	5.47	5.25
13	5.95	5.95	5.85	5.79	5.55	5.47	5.29
14	5.97	5.94	5.85	5.80	5.55	5.48	5.32
15	5.97	5.95	5.86	5.80	5.54	5.48	5.34
16	5.98	5.95	5.87	5.79	5.53	5.49	5.36
17	5.98	5.94	5.87	5.77	5.53	5.49	5.36
18	5.97	5.94	5.86	5.74	5.52	5.48	5.36
19	5.95	5.92	5.84	5.71	5.51	5.46	5.36
20	5.92	5.90	5.82	5.66	5.48	5.44	5.37
21	5.88	5.87	5.79	5.62	5.45	5.41	5.37
22	5.84	5.82	5.75	5.57	5.40	5.38	5.35
23	5.78	5.76	5.70	5.50	5.34	5.33	5.29
24	5.71	5.69	5.63	5.43	5.26	5.27	5.23
25	5.62	5.61	5.55	5.34	5.19	5.21	5.15
26	5.51	5.52	5.45	5.24	5.10	5.11	5.07
27	5.39	5.40	5.34	5.13	4.99	5.02	4.99
28	5.26	5.26	5.21	5.00	4.88	4.91	4.90
29	5.11	5.11	5.06	4.86	4.74	4.78	4.79
30	4.96	4.95	4.91	4.71	4.58	4.62	4.66
31	4.81	4.78	4.75	4.54	4.41	4.44	4.53
32	4.63	4.59	4.58	4.36	4.23	4.26	4.37
33	4.45	4.39	4.40	4.18	4.04	4.07	4.19
34	4.24	4.18	4.22	3.98	3.83	3.87	3.98
35	4.02	3.98	4.02	3.77	3.62	3.66	3.76
36	3.80	3.77	3.80	3.55	3.40	3.43	3.55
37	3.57	3.57	3.57	3.32	3.19	3.20	3.35
38	3.36	3.37	3.35	3.09	2.98	2.98	3.14
39	3.15	3.17	3.12	2.88	2.77	2.77	2.91
40	2.92	2.95	2.90	2.68	2.56	2.56	2.68
41	2.70	2.72	2.68	2.49	2.36	2.36	2.47
42	2.48	2.49	2.46	2.30	2.16	2.17	2.29
43	2.28	2.26	2.24	2.11	1.97	1.98	2.14
44	2.09	2.05	2.04	1.91	1.79	1.79	1.99
45	1.90	1.86	1.86	1.72	1.62	1.63	1.84
46	1.73	1.69	1.69	1.54	1.45	1.48	1.67
47	1.56	1.52	1.54	1.38	1.30	1.33	1.49
48	1.41	1.36	1.40	1.23	1.15	1.20	1.32
49	1.25	1.22	1.26	1.09	1.02	1.06	1.20
50	1.10	1.07	1.13	.96	.91	.95	1.08
51	.97	.94	1.01	.85	.80	.84	.97
52	.85	.81	.90	.74	.70	.75	.86
53	.74	.71	.80	.65	.60	.67	.75
54	.65	.65	.71	.56	.51	.60	.65
55	.57	.60	.62	.49	.44	.52	.55
56	.52	.53	.54	.43	.37	.45	.45
57	.46	.45	.48	.38	.31	.39	.39
58	.41	.38	.43	.34	.26	.34	.33
59	.34	.31	.38	.30	.22	.30	.29
60	.26	.25	.32	.27	.18	.25	.25

TABLE VIII.- MODEL ATMOSPHERES DERIVED FROM METEOROLOGICAL DATA

[From ref. 1]

Altitude, km	Cell 1 (58° N 68° W)		Cell 2 (53° N 60° W)		Cell 3 (47° N 57° W)		Cell 4 (43° N 45° W)	
	Temperature, °K	Pressure, mb	Temperature, °K	Pressure, mb	Temperature, °K	Pressure, mb	Temperature, °K	Pressure, mb
0	288.0	1010.000	288.0	1010.000	286.0	1012.000	294.0	1025.000
2	277.0	800.511	277.4	800.575	280.1	807.089	284.3	811.321
4	263.2	626.923	264.2	625.462	268.4	634.169	278.2	637.879
6	250.9	477.778	251.3	477.778	257.3	485.542	260.8	489.881
8	234.7	362.245	237.1	364.762	243.3	371.429	246.5	375.253
10	221.7	267.500	221.7	268.487	230.0	277.642	231.3	281.707
12	224.9	196.296	223.8	196.543	217.1	203.652	213.9	207.343
14	224.0	145.370	221.2	145.000	218.0	149.000	213.1	148.810
16	224.0	111.025	222.7	106.884	218.0	110.075	216.5	105.932
18	224.3	79.783	224.0	79.690	219.6	80.161	219.5	81.053
20	225.0	59.065	225.0	59.039	223.1	56.319	222.0	59.115
22	225.6	43.153	225.9	42.702	224.6	43.495	222.6	43.420
24	227.6	31.922	226.0	31.787	225.8	32.132	223.0	31.998
26	232.0	23.590	227.0	23.475	227.2	23.761	225.2	23.583
28	233.6	17.715	228.3	17.491	230.6	17.690	228.1	17.676
30	235.0	13.200	235.0	12.950	237.0	13.170	232.7	13.151
32	237.8	9.910	237.0	9.720	237.0	9.900	238.0	9.740
34	240.6	7.470	240.0	7.320	240.0	7.450	241.0	7.340
36	245.6	5.650	244.0	5.530	245.0	5.640	246.0	5.560
38	252.8	4.310	251.0	4.210	251.0	4.290	250.0	4.240
40	260.0	3.310	258.0	3.230	257.0	3.290	256.0	3.240
42	262.8	2.556	261.0	2.490	260.0	2.535	260.0	2.498
44	256.6	1.971	264.0	1.920	263.0	1.959	263.0	1.930
46	267.0	1.523	265.0	1.491	265.0	1.517	265.0	1.495
48	266.0	1.183	264.0	1.156	265.0	1.177	264.0	1.159
50	265.0	.918	263.0	.895	262.0	.911	262.0	.897
52	261.4	.710	259.0	.691	260.0	.704	261.0	.694
54	258.8	.548	256.0	.532	257.0	.543	260.0	.536
56	257.5	.442	254.7	.431	255.0	.439	257.0	.433
58	256.3	.336	253.3	.331	253.0	.334	254.0	.331
60	255.0	.230	252.0	.230	251.0	.230	251.0	.228
62	246.2	.180	244.4	.180	243.8	.179	243.0	.178
64	237.4	.130	236.8	.130	236.6	.128	235.0	.128
66	229.0	.095	229.0	.095	229.0	.093	227.6	.093
68	221.0	.074	221.0	.074	221.0	.073	220.8	.073
70	213.0	.053	213.0	.053	213.0	.053	214.0	.053

TABLE VIII.- MODEL ATMOSPHERES DERIVED FROM METEOROLOGICAL DATA – Concluded

[From ref. 1]

Altitude, km	Cell 5 (35° N 48° W)		Cell 6 (21° N 55° W)		Cell 7 (17° N 60° W)	
	Temperature, °K	Pressure, mb	Temperature, °K	Pressure, mb	Temperature, °K	Pressure, mb
0	299.0	1023.000	301.0	1016.000	301.0	1016.000
2	284.1	785.377	287.8	808.129	287.8	808.129
4	274.8	639.370	275.2	637.736	275.2	637.736
6	264.5	495.294	259.7	492.669	259.7	492.669
8	250.5	380.612	252.7	379.412	252.7	379.412
10	235.3	287.600	237.1	286.800	237.1	286.800
12	218.2	213.194	220.9	213.014	220.9	213.014
14	204.0	155.000	209.0	154.749	209.0	154.749
16	207.5	112.398	201.0	110.853	201.0	110.853
18	213.0	81.087	205.0	78.659	205.0	78.659
20	217.1	59.074	212.6	57.080	212.6	57.080
22	220.5	43.253	217.5	41.525	217.5	41.525
24	222.7	31.744	219.0	30.412	219.0	30.422
26	225.6	23.350	227.0	22.585	227.0	22.585
28	227.7	17.360	227.7	16.833	227.7	16.839
30	230.0	12.830	227.0	12.390	225.0	12.380
32	239.0	9.620	235.0	9.250	233.0	9.220
34	244.0	7.270	242.0	6.970	241.0	6.930
36	248.0	5.520	247.0	5.290	247.0	5.260
38	251.0	4.220	250.0	4.030	250.0	4.010
40	254.0	3.230	253.0	3.080	253.0	3.070
42	259.0	2.481	259.0	2.370	259.0	2.358
44	264.0	1.917	266.0	1.834	260.0	1.825
46	265.0	1.487	268.0	1.426	270.0	1.420
48	264.0	1.153	265.0	1.108	269.0	1.107
50	262.0	.893	262.0	.859	262.0	.859
52	265.0	.692	267.0	.666	268.0	.667
54	268.0	.538	273.0	.520	273.0	.520
56	264.0	.434	267.0	.422	266.3	.425
58	260.0	.329	261.0	.323	259.7	.330
60	256.0	.225	255.0	.225	253.0	.235
62	248.4	.181	247.8	.181	246.2	.189
64	240.8	.136	240.6	.136	239.4	.143
66	233.4	.102	233.2	.102	232.6	.108
68	226.2	.077	225.6	.077	225.8	.083
70	219.0	.053	218.0	.053	219.0	.058

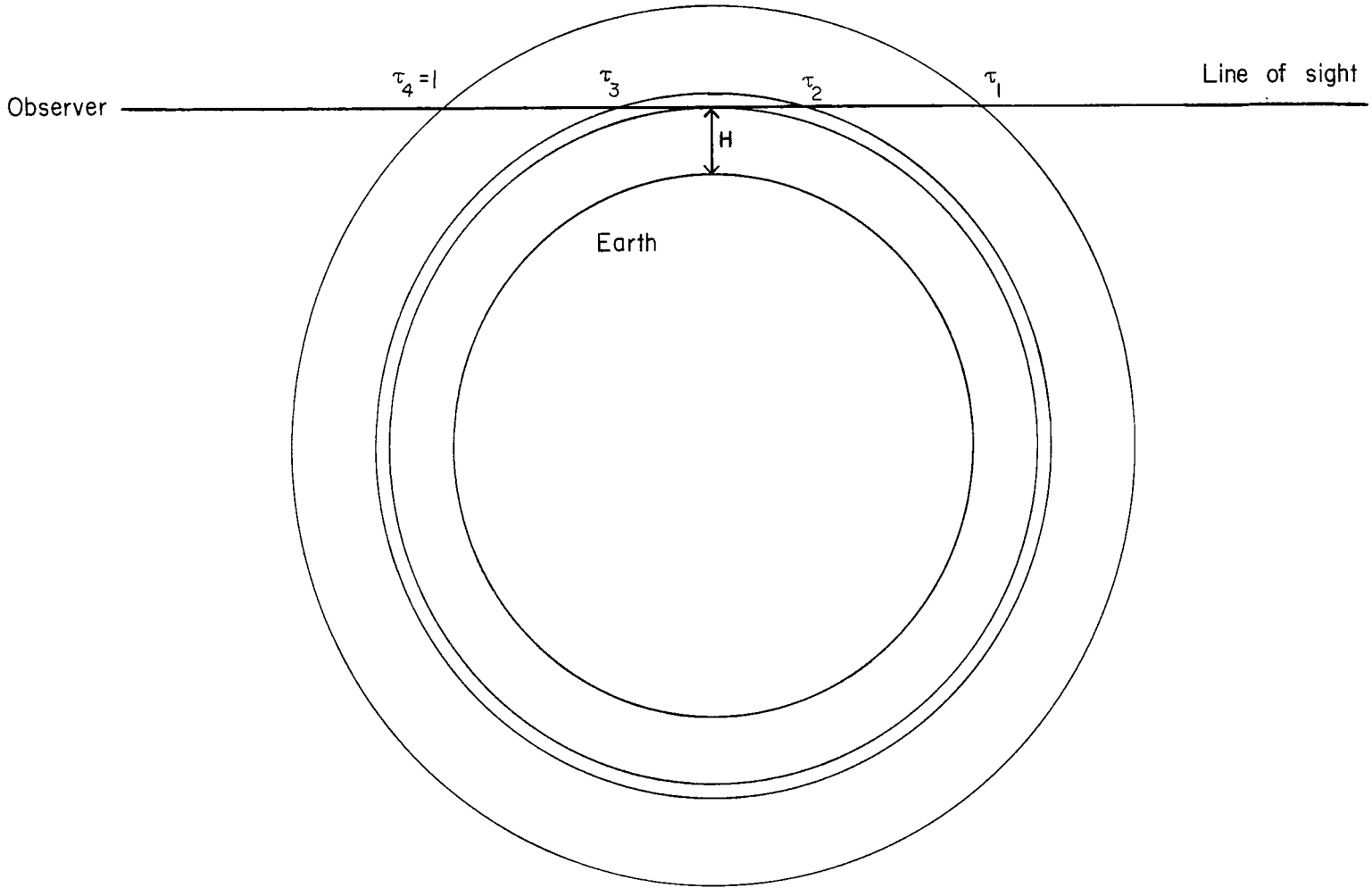

Figure 1.- Horizon geometry.

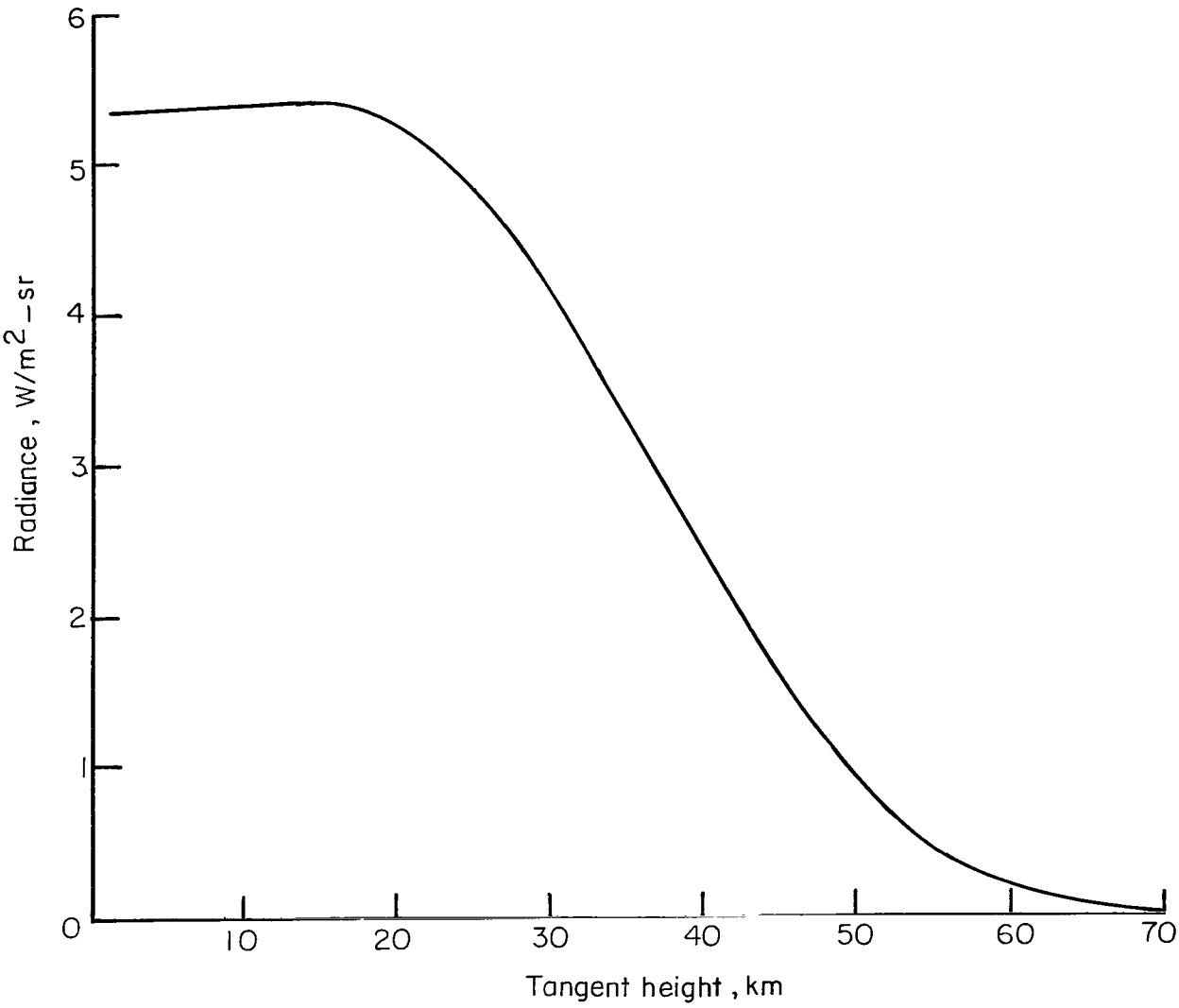

Figure 2.- Horizon radiance profile for 615 cm^{-1} to 715 cm^{-1} from 1962 U.S. Standard Atmosphere.

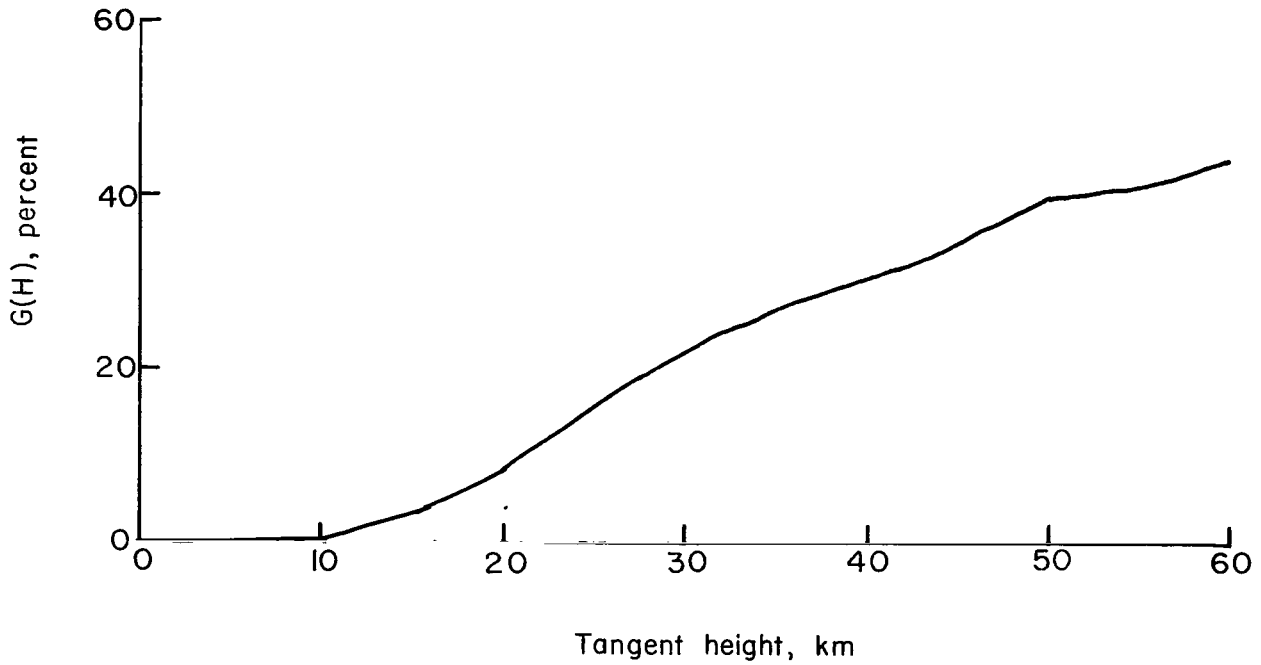

Figure 3.- Radiance contribution from 1-km layer above tangent point for spectral interval 615 cm^{-1} to 715 cm^{-1} and 1962 U.S. Standard Atmosphere.

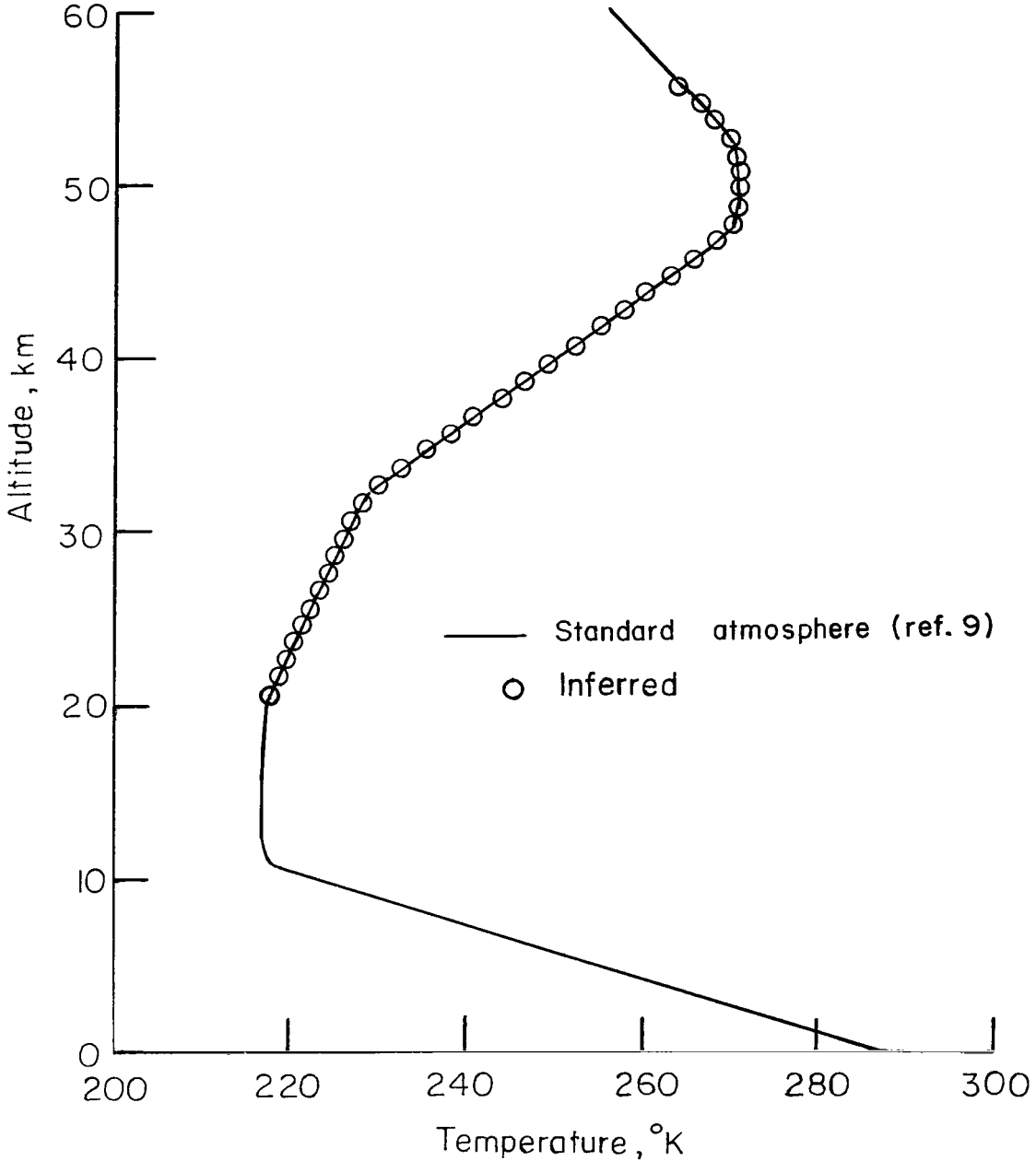

Figure 4.- Inferred temperature profile for perfect calculated radiance data.

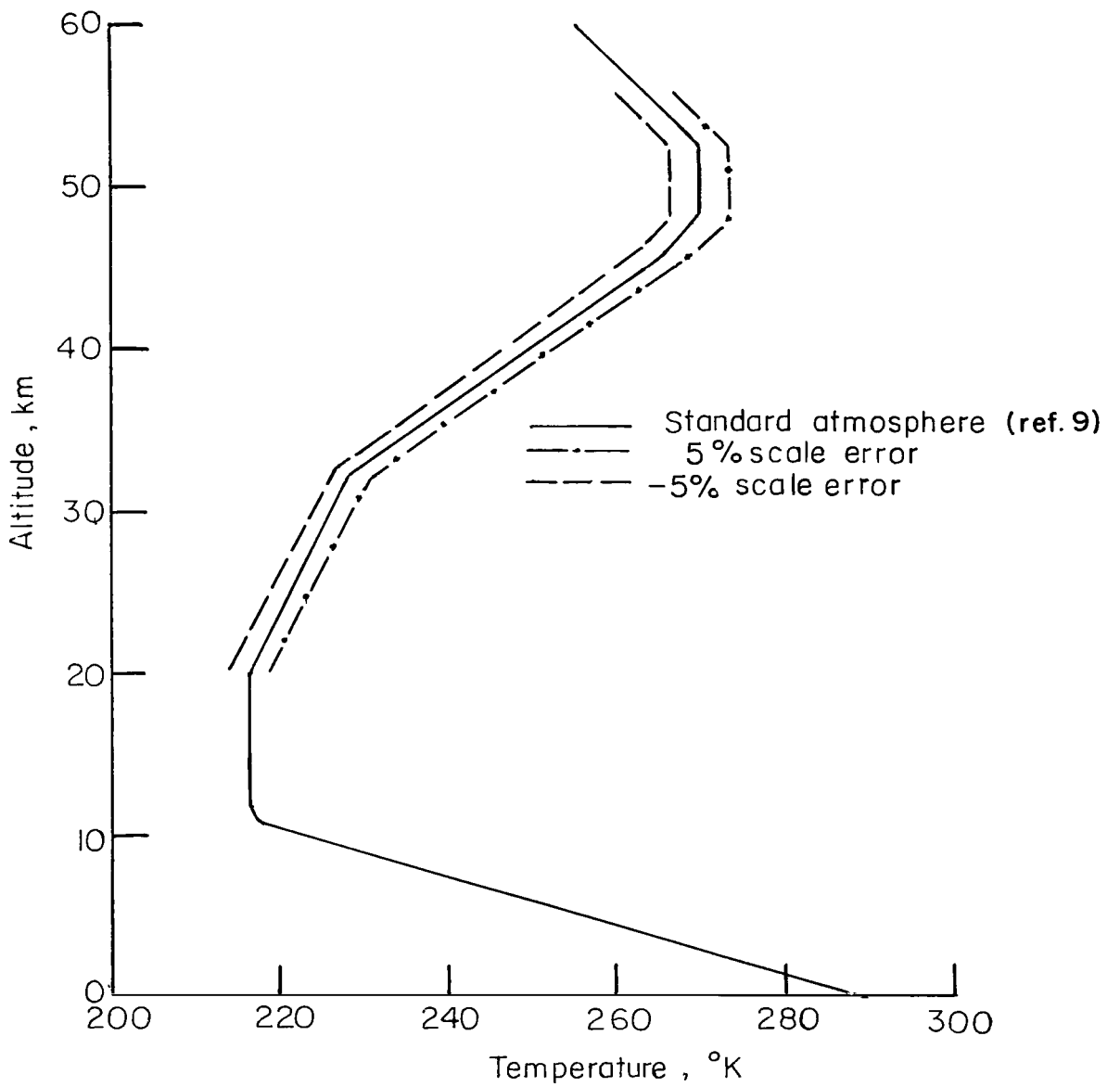

(a) Scale radiance errors.

Figure 5.- Inferred temperature profiles.

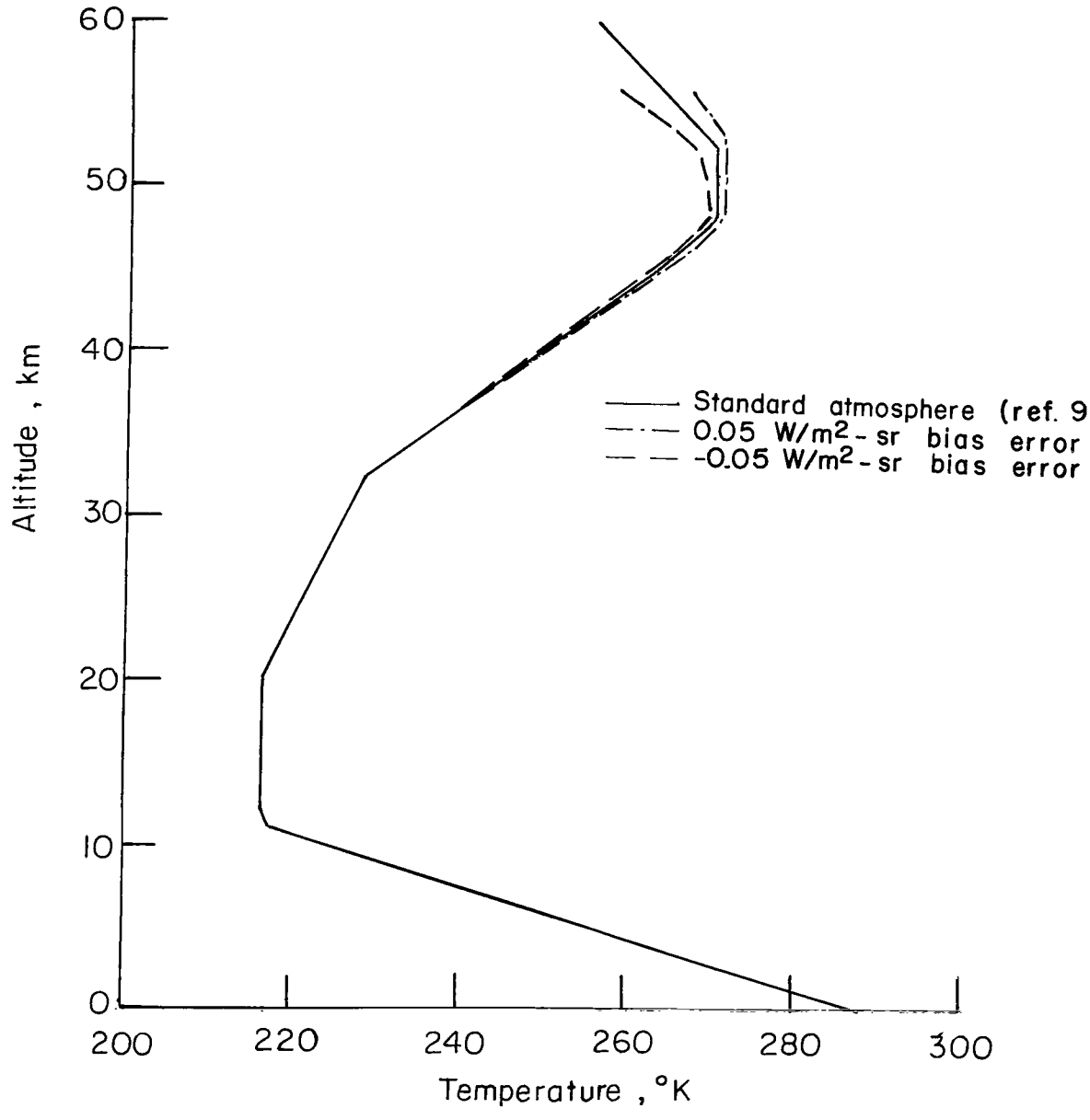

(b) Bias radiance errors.

Figure 5.- Continued.

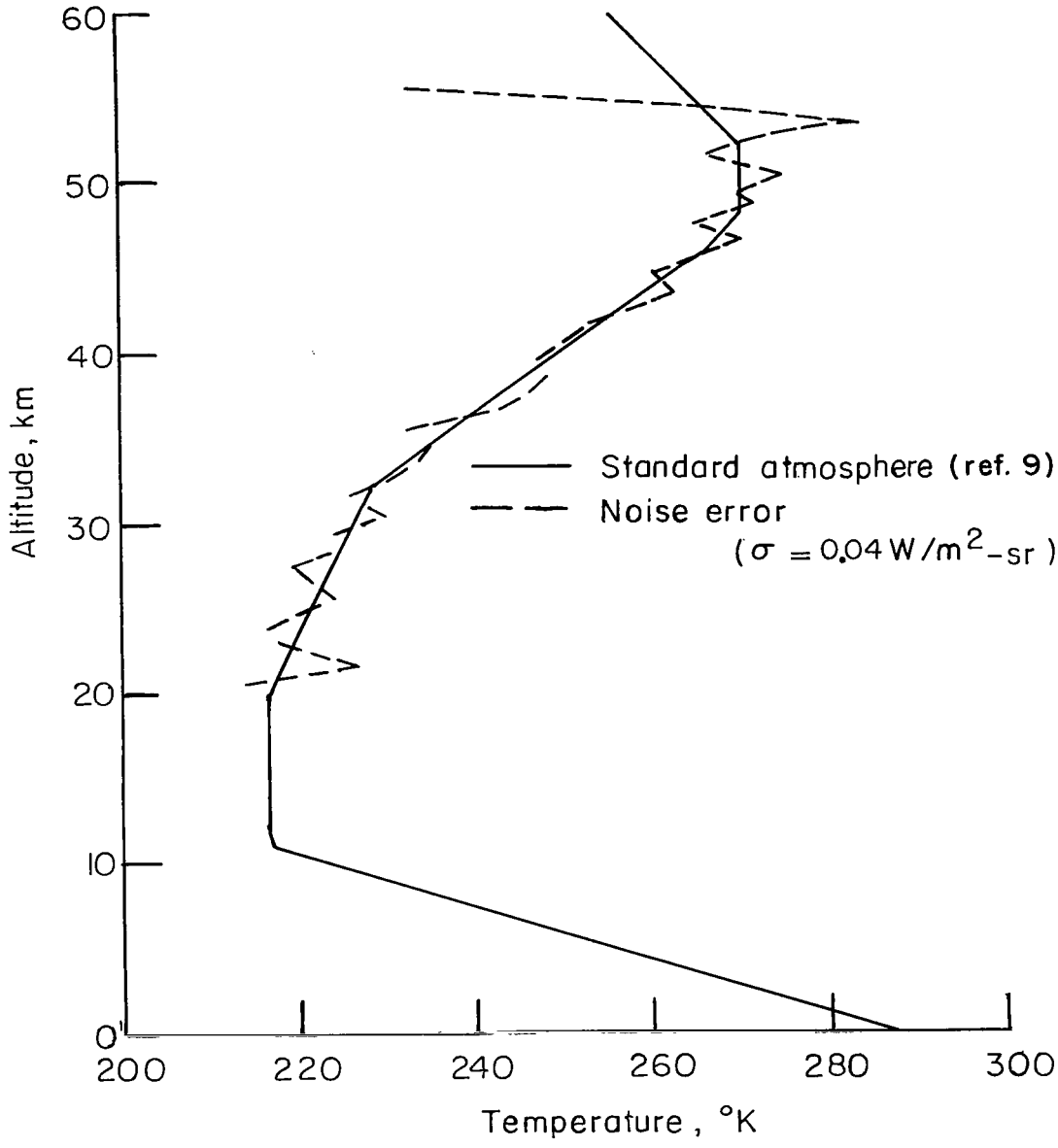

(c) Noise radiance errors.

Figure 5.- Continued.

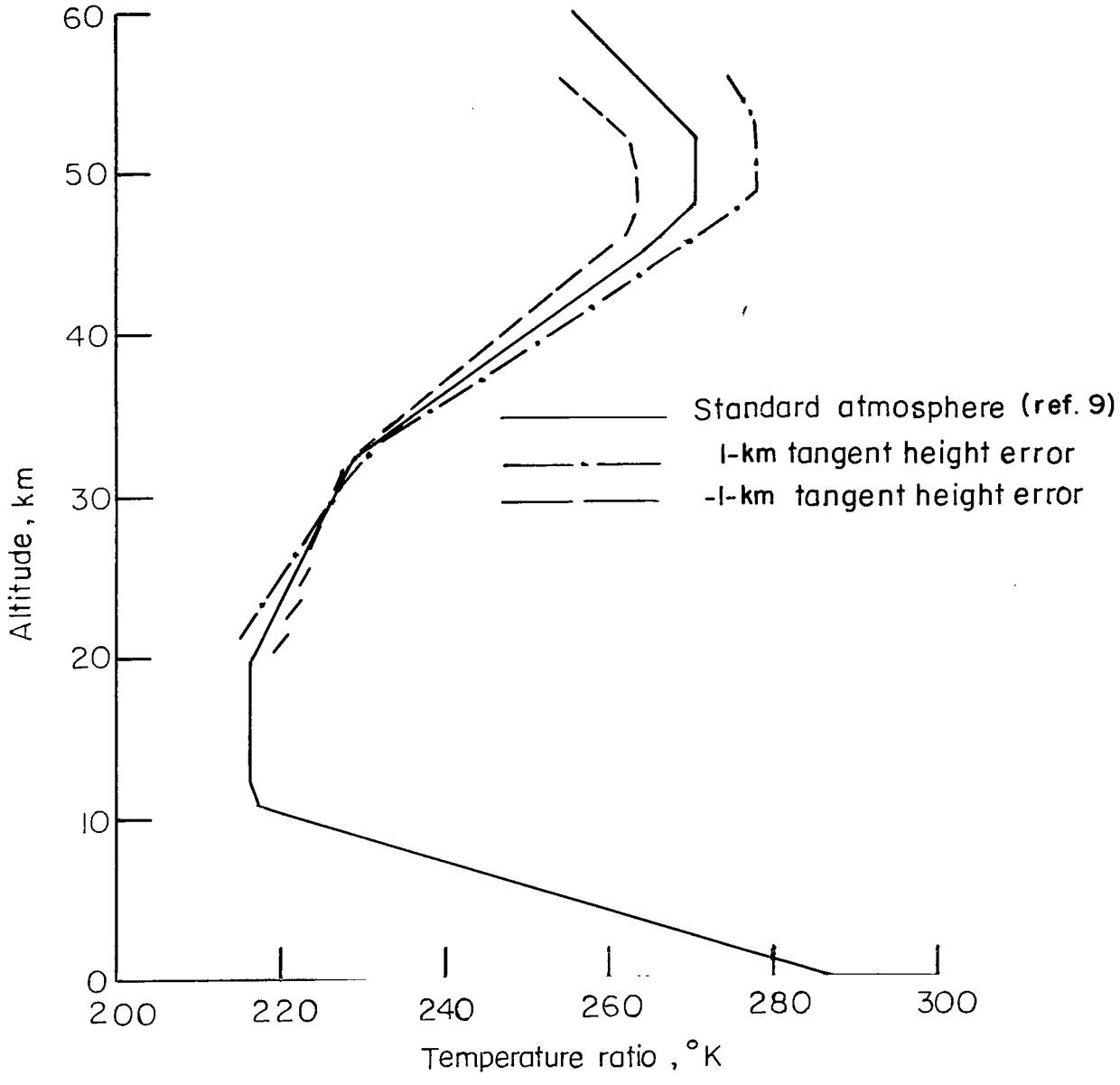

(d) Tangent height errors.

Figure 5.- Concluded.

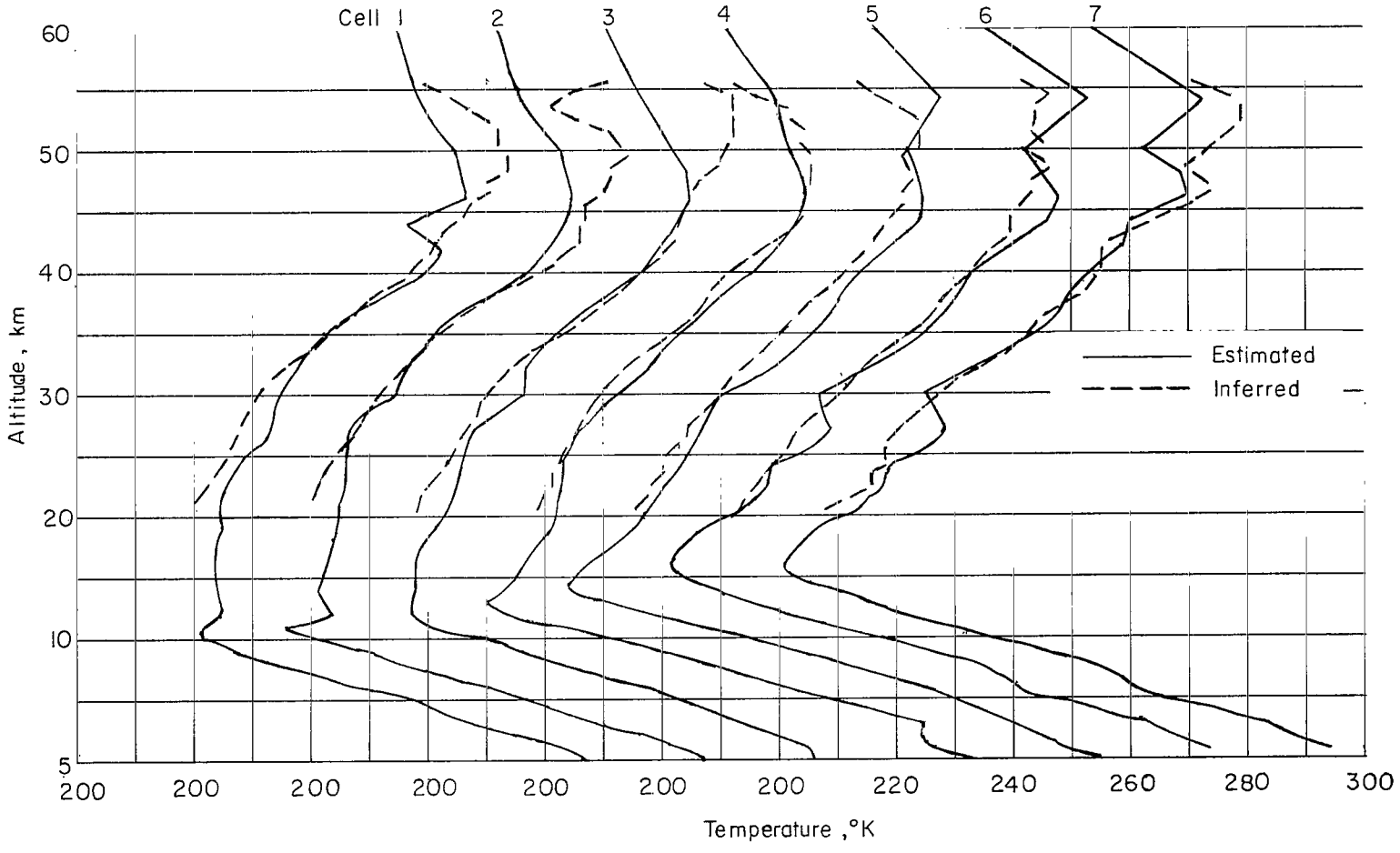

Figure 6.- Inferred and estimated temperature profiles for Project Scanner data.

"The aeronautical and space activities of the United States shall be conducted so as to contribute . . . to the expansion of human knowledge of phenomena in the atmosphere and space. The Administration shall provide for the widest practicable and appropriate dissemination of information concerning its activities and the results thereof."

—NATIONAL AERONAUTICS AND SPACE ACT OF 1958

NASA SCIENTIFIC AND TECHNICAL PUBLICATIONS

TECHNICAL REPORTS: Scientific and technical information considered important, complete, and a lasting contribution to existing knowledge.

TECHNICAL NOTES: Information less broad in scope but nevertheless of importance as a contribution to existing knowledge.

TECHNICAL MEMORANDUMS: Information receiving limited distribution because of preliminary data, security classification, or other reasons.

CONTRACTOR REPORTS: Scientific and technical information generated under a NASA contract or grant and considered an important contribution to existing knowledge.

TECHNICAL TRANSLATIONS: Information published in a foreign language considered to merit NASA distribution in English.

SPECIAL PUBLICATIONS: Information derived from or of value to NASA activities. Publications include conference proceedings, monographs, data compilations, handbooks, sourcebooks, and special bibliographies.

TECHNOLOGY UTILIZATION PUBLICATIONS: Information on technology used by NASA that may be of particular interest in commercial and other non-aerospace applications. Publications include Tech Briefs, Technology Utilization Reports and Notes, and Technology Surveys.

Details on the availability of these publications may be obtained from:

SCIENTIFIC AND TECHNICAL INFORMATION DIVISION

NATIONAL AERONAUTICS AND SPACE ADMINISTRATION

Washington, D.C. 20546